Title

Enhancing antibody responses by multivalent antigen display on thymus-independent DNA origami scaffolds

Authors

Eike-Christian Wamhoff[1,*], Larance Ronsard[2,*], Jared Feldman[2,*], Blake M. Hauser[2,*] Grant A. Knappe[1,3], Anna Romanov[1,4], Evan Lam[2], Kerri St. Denis[2], Alejandro B. Balazs[2], Aaron Schmidt[2,5**], Daniel Lingwood[2,**] and Mark Bathe[1,**]

[1]Department of Biological Engineering, Massachusetts Institute of Technology, Cambridge, MA 02139, United States

[2]Ragon Institute of Massachusetts General Hospital, Massachusetts Institute of Technology and Harvard University, Cambridge, MA 02139, United States

[3]Department of Chemical Engineering, Massachusetts Institute of Technology, Cambridge, MA 02139, United States

[4]Koch Institute for Integrative Cancer Research, Massachusetts Institute of Technology, Cambridge, MA 02139, United States

[5]Department of Microbiology, Harvard Medical School, Boston, MA 02115, United States

*These authors contributed equally

**Correspondence to: mark.bathe@mit.edu, dlingwood@mgh.harvard.edu or aschmidt@crystal.harvard.edu

Abstract

Multivalent antigen display is a well-established design principle to enhance humoral immunity elicited by subunit vaccines. Protein-based virus-like particles (VLPs) are an important vaccine platform that implements this principle but also contain thymus-dependent off-target epitopes, thereby generating neutralizing and defocused antibody responses against the scaffold itself. Here, we present DNA origami as an alternative platform to display the receptor binding domain (RBD) of SARS-CoV-2. DNA-based scaffolds provide nanoscale control over antigen organization and, as thymus-independent antigens, are expected to induce only extrafollicular B-cell responses. Our icosahedral DNA-based VLPs elicited valency-dependent BCR signaling in two reporter B-cell lines, with corresponding increases in RBD-specific antibody responses following sequential immunization in mice. Mouse sera also neutralized the Wuhan strain of SARS-CoV-2—but did not contain boosted, DNA-specific antibodies. Thus, multivalent display using DNA origami can enhance immunogenicity of protein antigens without generating scaffold-directed immunological memory and may prove useful for rational vaccine design.

Introduction

The multivalent display of antigens at the nanoscale has been demonstrated to improve the immunogenicity of subunit vaccines[1-3]. Nanoparticulate vaccines with diameters between 20 and 200 nm ensure efficient trafficking to secondary lymphoid organs[4]. In secondary lymphoid organs, high valency and avidity promote B-cell receptor (BCR) crosslinking and signaling as well as BCR-mediated antigen uptake, thereby driving early B-cell activation and humoral immunity[5-12]. The importance of BCR signaling for antibody responses was initially recognized for thymus-independent (TI) antigens, particularly of the TI-2 class[13-15]. The multivalent display of these non-protein antigens induces BCR crosslinking in the absence of T-cell help, ensuring that antibody responses proceed through extrafollicular B-cell pathways and thereby limiting germinal center (GC) reactions, affinity maturation and induction of B-cell memory[16-17]. Multivalent antigen display also enhances the BCR-mediated response to thymus-dependent (TD) antigens including proteins[7-8]. In this context, follicular T-cell help enables GC reactions to generate affinity-matured B-cell memory that can be boosted or recalled upon antigen reexposure[18-20]. Consequently, the nanoscale organization of antigens represents a well-established vaccine design principle, not only for TI antigens, but also to elicit humoral immunity through the TD pathway[1-3].

Leveraging this design principle, native and engineered protein-based virus-like particles (P-VLPs) have emerged as an important platform for multivalent subunit vaccines[21-36]. P-VLPs enable the rigid display of antigens and have recently been used to investigate the impact of valency on B-cell activation *in vivo* to greater detail, suggesting differential regulation of affinity maturation and enhanced breadth of antibody responses at high valency[7-9]. However, valency control remains limited by the number of distinct protein components used for VLP assembly or by statistical functionalization with antigens—and is typically dependent on scaffold size and geometry. Notably, protein-based scaffolds are also TD antigens that elicit humoral immunity, including both T- and B-cell memory[36-37]. These scaffolds contain, and multivalently display, off-target epitopes that can defocus antibody responses, and such defocusing competes with the principles of rational vaccine design[38-39]. Scaffold-directed immunological memory can further complicate sequential or diversified immunizations with a given P-VLP, resulting in antibody-dependent clearance of the vaccine platform[40-41].

We sought to address these limitations by combining rigid, multivalent antigen display with scaffolds composed of TI antigens. We hypothesized that such nanoscale organization could promote TD antibody responses against protein antigens but confine scaffold-directed B-cell responses to the non-boostable, extrafollicular pathway devoid of immunological memory. Wireframe DNA origami provides access to designer VLPs of controlled geometry and size at the 20 to 200 nm scale with independently programmable geometry, valency and stoichiometry of antigen display[42-46]. We and others recently leveraged this platform to probe the nanoscale parameters of IgM recognition and of BCR signaling in reporter B-cell lines, suggesting that increased antigen spacing up to 30 nm promotes early B-cell activation[47-48]. However, these nanoscale design rules remain to be validated *in vivo*. While the utility of DNA-based VLPs (DNA-VLPs) to enhance antibody responses has not been demonstrated, DNA origami has been successfully employed to deliver therapeutic cargo to tumors in mice[49-50]. Other examples of *in vivo* delivery include the co-formulation of antigens and adjuvants to elicit T-cell immunity[51]. Importantly, and in contrast to P-VLPs, DNA-based scaffolds constitute TI antigens and should therefore be excluded from the boostable follicular pathway[51-52].

As proof-of-concept, we report on the fabrication of DNA-VLPs functionalized with the SARS-CoV-2 receptor binding domain (RBD) derived from the spike glycoprotein, a key target for eliciting neutralizing antibodies against the virus[53-56]. Our nanoparticulate vaccine displayed enhanced binding to ACE2-expressing cells and induced valency-dependent BCR signaling *in vitro*. Following sequential immunization in mice, we observed corresponding valency-dependent enhancement of RBD-specific antibody responses and B-cell memory recall. Mouse sera also efficiently neutralized the Wuhan strain of SARS-CoV-2 for DNA-VLPs compared with monomeric RBD—but did not contain boosted, DNA-specific antibodies. Taken together, our findings suggest that DNA origami can be leveraged for multivalent antigen display without eliciting TD B-cell responses against the DNA-based scaffold, rendering this platform useful for rational vaccine design.

Results and Discussion

The spherical SARS-CoV-2 virion is approximately 100 nm in diameter and displays approximately 100 trimeric spike glycoproteins[57]. Each monomer contains the RBD which is essential for engaging the ACE2 receptor and viral uptake, rendering it a key target of neutralizing antibody responses[53-56]. We adapted our previous DAEDALUS design, an icosahedral DNA-VLP with 50 potential conjugation sites and approximately 34 nm in diameter, to display the RBD and investigate impact of nanoscale antigen organization by DNA origami on B-cell activation[48]. A covalent *in situ* functionalization strategy employing strain-promoted azide-alkyne cycloaddition (SPAAC) chemistry was used for antigen attachment (**Figure 1A**)[44]. Towards this end, we synthesized 30 oligonucleotide staples bearing triethylene glycol (TEG)-DBCO groups at their 5' ends to assembly DNA-VLPs symmetrically displaying 1x, 6x or 30x DBCO groups on their exterior (**Figure S1**, **Table S1 to S3**). Employing a reoxidation strategy, the RBD was selectively modified at an engineered C-terminal Cys with a SMCC-TEG-azide linker and subsequently incubated with DBCO-bearing DNA origami to fabricate **I52-1x-, 6x-, 30x-RBD** (**Figures 1B and S2**, **Note S1**). The optimization of reaction conditions yielded near-quantitative conversion and coverage of more than 80% of conjugation sites on average as determined by denaturing, reversed-phase HPLC and Trp fluorescence (**Figures 1C and S3**). Notably, conversion was dependent on maximum DBCO concentrations and we obtained only up to 30% coverage for **I52-1x-RBD**. The monodispersity of purified DNA-VLPs was validated by dynamic light scattering (DLS) (**Figure 1D**). Analysis of **I52-30x-RBD** via negative-strain transmission electron microscopy (TEM) validated structural integrity of the DNA origami (**Figure 1E and S4**). While the icosahedral geometry could not be fully resolved, presumably due to accumulation of uranyl formate in the interior of the DNA origami, antigens were clearly visible and organized symmetrically.

To investigate the binding activity of RBD-Az before and after conjugation to DNA-VLPs, we conducted flow cytometry experiments with ACE2-expressing HEK293 cells (**Figure 2A**). Initially, monovalent binding of wild-type RBD and fluorophore-labeled RBD-Cy5, obtained by selectively labeling the azide, was compared (**Figure 2B and C**). The RBD constructs were incubated at 200 nM with the HEK293 cells and bound antigen was detected using the previously described anti-RBD antibody CR3022[56]. These experiments revealed comparable binding between the two constructs, demonstrating preservation of the receptor binding motif (RBM) and the viability of the reoxidation strategy for selective labeling of the terminal Cys (**Figure S2, Note S1**). Next, we explored whether multivalent RBD display using DNA-VLPs would result in increased avidity. Two additional fluorophore-labeled VLPs, **I52-30x-RBD-5x-Cy5** and **I52-5x-Cy5**, were synthesized to allow for direct detection of binding (**Figure 1B and S1**). Indeed, binding

of the RBD-functionalized VLPs was significantly enhanced compared to monomeric RBD-Cy5, while no binding was observed for the **I52-5x-Cy5** (**Figure 2D and E**). When correcting for Cy5 brightness per RBD, **I52-30x-RBD-5x-Cy5** displayed approximately one order of magnitude higher median fluorescence intensity compared with monomeric RBD-Cy5, indicative of avidity effects for VLP recognition**.**

We then evaluated the capacity of RBD-functionalized DNA-VLPs to induce BCR signaling using a previously described Ca^{2+} flux assay (**Figure 2A**)[58]. Specifically, Ramos B-cell lines expressing the somatic CR3022 or B38 antibodies were established[56, 59]. BCR signaling was initially validated by incubation with an anti-IgM antibody. At 30 nM antigen, monomeric wild-type RBD did not elicit B-cell activation *in vitro* (**Figure 2F and G**). By contrast, incubation of the Ramos B cells with multivalent DNA-VLPs at the same antigen concentration resulted in efficient BCR signaling. We further observed valency-dependent increases in total Ca^{2+} flux for both cell lines with **I52-30x-RBD** being more potent than **I52-6x-RBD**. CR3022 (K_D = 0.27 μM, **Figure 2F**) and B38 (K_D = 1.00 μM, **Figure 2G**) bind distinct RBD epitopes with moderate monovalent affinity as reported for the corresponding Fab fragments[60]. Despite this 4-fold difference in affinity, we observed comparable total BCR signaling relative to the IgM control for all functionalized DNA-VLPs, consistent with previously described avidity effects at the B-cell surface[61]. We concluded that our DNA-VLPs efficiently interacted with and induced signaling by RBD-specific BCRs, analogous to previous studies using similar assays to evaluate multivalent subunit vaccines[58, 62-68]. The increased B-cell activation for **I52-30x-RBD** contrasts our previous findings for HIV antigens for which total Ca^{2+} flux saturated beyond a valency of 10x[48]. Notably, the antigen-BCR systems differ with respect to affinity and mode of antigen attachment: The affinity of the HIV antigen was substantially higher (eOD-GT8, K_D = 30 pM) and the antigens were non-covalently attached to DNA origami using rigid DNA-PNA duplexes.

Next, we investigated whether RBD-functionalized DNA-VLPs could activate B-cells *in vivo* and induce antibody responses. C57BL/6 mice were sequentially immunized with monomeric wild-type RBD, **I52-6x-RBD** and **I52-30x-RBD** at doses equivalent to 7.5 μg RBD (**Figure 3A and S3**). IgG responses against the RBD were monitored throughout this regimen using ELISA and correlated with our *in vitro* BCR signaling findings (**Figure 3B and S5**). Post-boost 1, we observed an approximately 130-fold increase in endpoint dilutions for the 30-valent DNA-VLP over monomeric RBD. **I52-6x-RBD** did not enhance the B-cell response and elicited comparable antibody titers to monomeric RBD, both post-boost 1 and 2. Overall, endpoint dilutions were further increased post-boost 2 but converged between the groups. Earlier and stronger boosting of IgG titers and efficient B-cell memory recall is a hallmark of multivalent versus monomeric subunit vaccines[22-23]. Our findings are further consistent with enhanced IgG titers elicited by P-VLPs of increasing the valency[7-9]. Notably, we did not observe boosting of DNA-specific IgG titers against the scaffold, indicating an absence of B-cell memory for the DNA-VLP (**Figure 3C and S6**). While this finding was expected for TI antigens such as DNA, it was also established that TD antibody responses can be generated against TI antigens by covalent attachment to protein antigens[69-70]. The inverse case does not appear to be the default—scaffolding protein antigens with TI antigens does not direct the B-cell response to the extrafollicular pathway. By contrast, we observed valency-dependent TD antibody responses to the RBD, akin to virosomal and ISCOM-based vaccine design principles in which protein antigens are multivalently displayed by TI antigen-composed matrices[71-74]. The valency-dependent enhancement of RBD-specific antibody responses was further reflected in the efficient neutralization of the wild-type, Wuhan strain of

SARS-CoV-2 (**Figure 3D**)[75-76]. These findings suggest that immunization with **I52-30x-RBD** not only resulted in increased IgG titers but also induced functionally improved humoral immunity.

Conclusions

Here, we report on the use of wireframe DNA origami to program the display of SARS-CoV-2 antigens. RBD-functionalized DNA-VLPs efficiently bound to the ACE2 receptor and activated B cells *in vitro*. BCR signaling increased with DNA-VLP valency and no saturation effects were observed for up to 30x RBD antigens. We further demonstrate the utility of DNA-VLPs as an *in vivo* platform for rational vaccine design. In particular, we provide proof-of-concept that multivalent DNA-VLPs can enhance TD antigen-specific humoral immunity in mice, but, as TI scaffolds, do not generate boostable B-cell memory against the vaccine platform itself. Because DNA origami also offers independent control over VLP size and geometry versus multivalent antigen display, DNA-based scaffolds may prove particularly useful if epitope focusing and nanoscale control are desired. By contrast, several P-VLPs explored as multivalent subunit vaccines against SARS-CoV-2 and other viruses elicit scaffold-directed humoral immunity[30-31, 36-37]— and the defocusing of RBD-specific antibody responses has been shown to reduce cross-neutralization of SARS-CoV-2 variants[37].

Maintaining antigen display in B-cell follicles over time has been shown to promote GC reactions and humoral immunity[77-78]. While our findings suggest that non-protected, covalently functionalized DNA-VLPs are sufficiently stable to enhance antibody responses, it will thus be important to investigate to what extent multivalent antigen display is maintained in secondary lymphoid organs in the presence of nuclease degradation[79-80]. Trafficking to secondary lymphoid organs and B-cell activation might also be enhanced by varying DNA-VLP size and valency, for example to mimic SARS-CoV-2 virions[57]. Beyond vaccine design, our findings are of potential importance to gene therapy by addressing antibody-dependent clearance[40-41]—with DNA origami emerging as an alternative delivery platform[81].

Methods

Methods are described in the **Supporting Information**.

Acknowledgments

E.-C.W., G.K., and M.B. were supported by NIH R21-EB026008, NSF CCF-1564025, CBET-1729397, and CCF-1956054, ONR N00014-21-1-4013 and N00014-17-1-2609, ARO ISN W911NF-13-D-0001, and Fast Grants Agreement EFF 4/15/20. E.-C. W. was additionally supported by the Feodor Lynen Fellowship of the Alexander von Humboldt Foundation. B.M.H was supported by NIGMS (T32GM007753) and F30 AI160908. J.F. was supported by NIGMS (T32AI007245). A.G.S. was supported by NIH (R01 AI146779) and a Massachusetts Consortium on Pathogenesis Readiness (MassCPR) grant. DL was supported by NIH (R01AI137057, R01AI153098, R01AI155447).

Figures

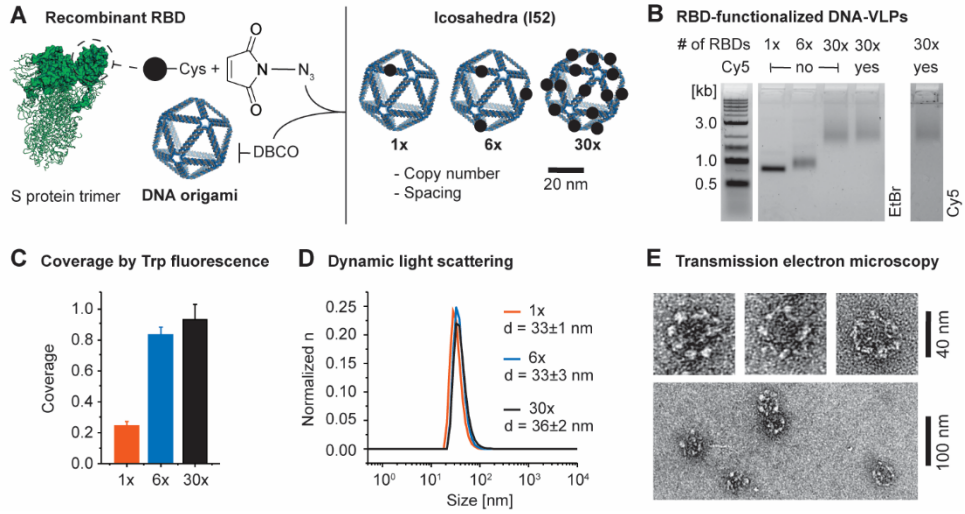

Figure 1. Design and synthesis of DNA-VLPs covalently displaying the SARS-CoV-2 RBD. **(A)** Recombinant RBD bearing an additional Cys residue at the C-terminus was expressed. The C-terminal Cys was selectively labeled with and SMCC-TEG-azide linker and subsequently conjugated to DBCO-bearing DNA-VLPs. The icosahedral DNA origami objects of approximately 50 nm diameter displaying 1, 6 and 30 copies of the RBD were fabricated. **(B)** Agarose gel electrophoresis (AGE) shows the gel shift due to increasing RBD copy number as well as low polydispersity of the VLPs samples after purification. An additional VLP bearing 5 copies of Cy5 was produced for ACE2-binding flow cytometry experiments. **(C)** The coverage of the DNA-VLPs with RBD was quantified via Trp fluorescence. **(D)** Dynamic light scattering (DLS) was used to assess the dispersity of functionalized VLP samples. Representative histograms are shown**. (E)** Transmission electron micrographs (TEM) of **I52-30x-RBD** were obtained by negative staining using 2% uranyl formate and validate the symmetric nanoscale organization of antigens. Coverage values were determined from n = 3 biological replicates for **I52-1x-RBD** and from n = 6 biological replicates for **I52-6x** and **30x-RBD**. Diameters were determined from 3 technical replicates.

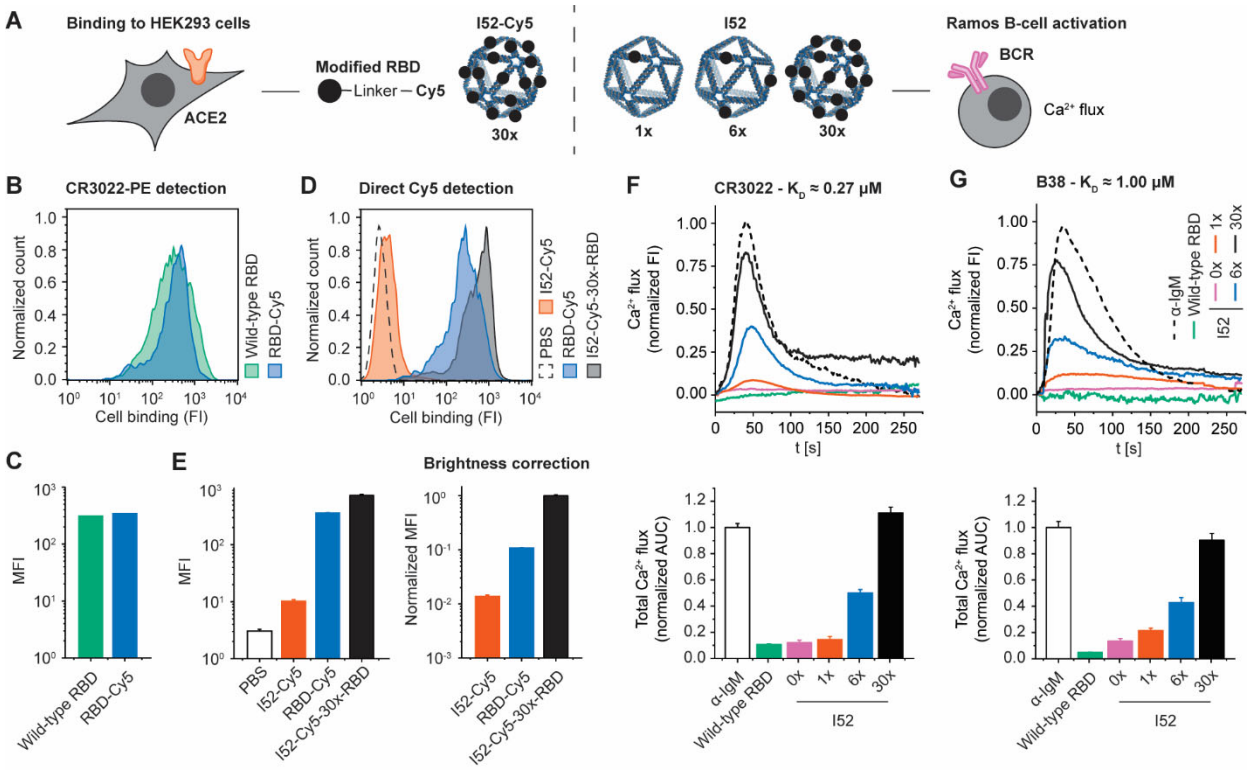

Figure 2. In vitro activity of RBD-functionalized DNA-VLPs.
(A) An overview of the in vitro activity assays and corresponding DNA-VLPs is shown. **(B and C)** ACE2-expressing HEK293 cells were incubated with 200 nM RBD. Binding was detected in flow cytometry experiments using PE-labeled CR3022 and a PE-labeled secondary antibody, demonstrating preserved binding activity for chemically modified RBD-Cy5 compared to wild-type RBD. **(D and E)** Incubation with Cy5-labeled **I52-30x-RBD** at 100 nM RBD revealed enhanced binding compared to RBD-Cy5 due to multivalency effects. No unspecific binding for non-functionalized **I52** was observed. The brightness of Cy5-labeled **I52-30x-RBD** (5 Cy5 per 30 RBDs) and RBD-Cy5 (1 Cy5 per 1 RBD) was quantified experimentally (**Figure S4**) and MFI values were corrected accordingly. **(F and G)** Ramos B cells expressing the BCRs C3022 and B38 were incubated with α-IgM, wild-type RBD or RBD-functionalized DNA-VLPs at 30 nM RBD. Ca^{2+} flux in response to RBD incubation was assayed using Fura Red. Representative fluorescence intensity curves are shown (top). Total Ca^{2+} flux was quantified via the normalized AUC, revealing robust activation of BCR-expressing Ramos B cells by functionalized DNA-VLPs (bottom). No stimulation was observed for wild-type RBD or for non-functionalized **I52**. Representative histograms are shown for ACE2 binding assays and MFI values were determined from n = 3 biological replicates. Normalized AUC values were determined from n = 3 biological replicates.

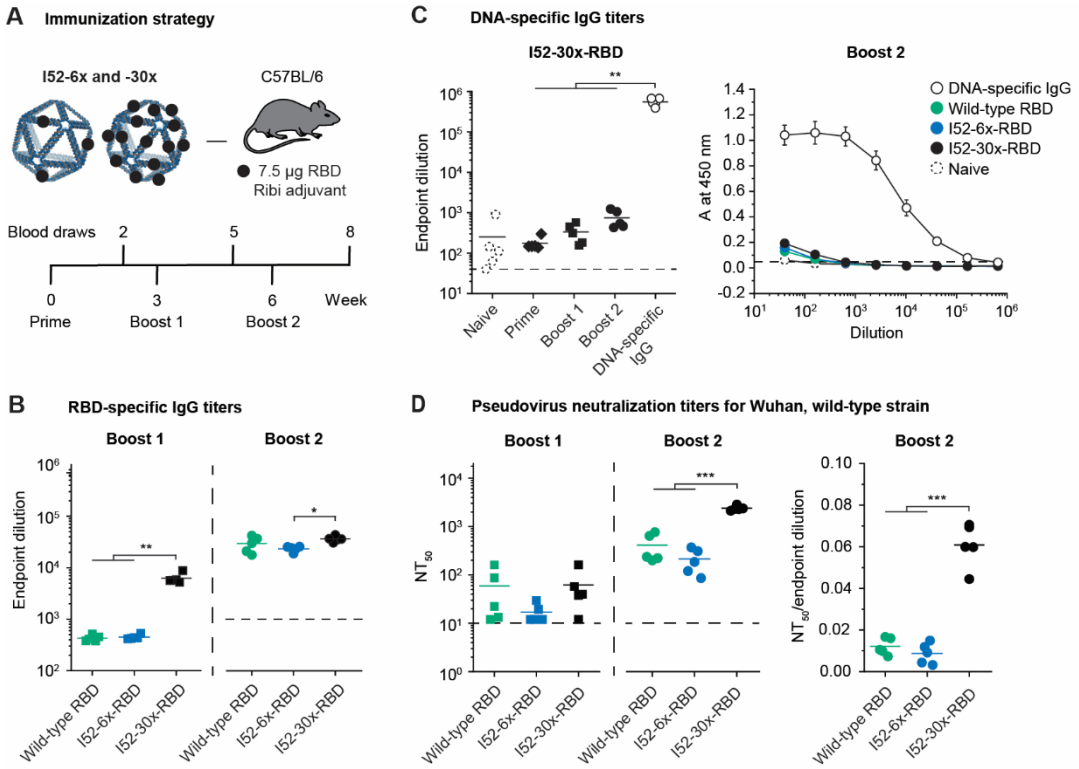

Figure 3. Antibody responses to RBD-functionalized DNA-VLPs.
(A) Mice were immunized intraperitoneally with monomeric RBD and RBD-functionalized DNA-VLPs of varying copy number following a prime-boost-boost regimen. **(B)** RBD-specific IgG endpoint dilutions were determined via ELISA, revealing enhanced antibody responses for **I52-30x-RBD** compared to both monomeric RBD and **I52-6x-RBD. (C)** DNA-VLPs did not elicit enhanced DNA-specific IgG titers compared to monomeric RBD as measured by ELISA. Importantly, DNA-specific IgG were not increased after boost immunizations with DNA-VLPs. DNA-specific IgG was diluted from 10 µg/ml. **(D)** Serum neutralization titers expressed as NT_{50} values against pseudoviruses modeling the wild-type, Wuhan strain were determined. We observed enhanced, valency-dependent neutralization efficiency for **I52-30x-RBD.** Mice were immunized with 7.5 ug RBD. IgG titers, RBD-specific IgG B cell fractions and NT_{50} values were determined from n = 5 biological replicates. One-way ANOVA was performed followed by Dunnett's T3 multiple comparison test at α = 0.05.

References

1. Singh, A., Eliciting B Cell Immunity against Infectious Diseases Using Nanovaccines. *Nat Nanotechnol* **2021,** *16* (1), 16-24.
2. Irvine, D. J.; Read, B. J., Shaping Humoral Immunity to Vaccines through Antigen-Displaying Nanoparticles. *Curr Opin Immunol* **2020,** *65*, 1-6.
3. Nguyen, B.; Tolia, N. H., Protein-Based Antigen Presentation Platforms for Nanoparticle Vaccines. *NPJ Vaccines* **2021,** *6* (1), 70.
4. Zhang, Y. N.; Lazarovits, J.; Poon, W.; Ouyang, B.; Nguyen, L. N. M.; Kingston, B. R.; Chan, W. C. W., Nanoparticle Size Influences Antigen Retention and Presentation in Lymph Node Follicles for Humoral Immunity. *Nano Lett* **2019,** *19* (10), 7226-7235.
5. Batista, F. D.; Iber, D.; Neuberger, M. S., B Cells Acquire Antigen from Target Cells after Synapse Formation. *Nature* **2001,** *411* (6836), 489-94.
6. Abbott, R. K.; Lee, J. H.; Menis, S.; Skog, P.; Rossi, M.; Ota, T.; Kulp, D. W.; Bhullar, D.; Kalyuzhniy, O.; Havenar-Daughton, C.; Schief, W. R.; Nemazee, D.; Crotty, S., Precursor Frequency and Affinity Determine B Cell Competitive Fitness in Germinal Centers, Tested with Germline-Targeting Hiv Vaccine Immunogens. *Immunity* **2018,** *48* (1), 133-146 e6.
7. Marcandalli, J.; Fiala, B.; Ols, S.; Perotti, M.; de van der Schueren, W.; Snijder, J.; Hodge, E.; Benhaim, M.; Ravichandran, R.; Carter, L.; Sheffler, W.; Brunner, L.; Lawrenz, M.; Dubois, P.; Lanzavecchia, A.; Sallusto, F.; Lee, K. K.; Veesler, D.; Correnti, C. E.; Stewart, L. J.; Baker, D.; Lore, K.; Perez, L.; King, N. P., Induction of Potent Neutralizing Antibody Responses by a Designed Protein Nanoparticle Vaccine for Respiratory Syncytial Virus. *Cell* **2019,** *176* (6), 1420-1431 e17.
8. Kato, Y.; Abbott, R. K.; Freeman, B. L.; Haupt, S.; Groschel, B.; Silva, M.; Menis, S.; Irvine, D. J.; Schief, W. R.; Crotty, S., Multifaceted Effects of Antigen Valency on B Cell Response Composition and Differentiation in Vivo. *Immunity* **2020,** *53* (3), 548-563 e8.
9. He, L.; Lin, X.; Wang, Y.; Abraham, C.; Sou, C.; Ngo, T.; Zhang, Y.; Wilson, I. A.; Zhu, J., Single-Component, Self-Assembling, Protein Nanoparticles Presenting the Receptor Binding Domain and Stabilized Spike as Sars-Cov-2 Vaccine Candidates. *Sci Adv* **2021,** *7* (12).
10. Batista, F. D.; Harwood, N. E., The Who, How and Where of Antigen Presentation to B Cells. *Nat Rev Immunol* **2009,** *9* (1), 15-27.
11. Kwak, K.; Akkaya, M.; Pierce, S. K., B Cell Signaling in Context. *Nat Immunol* **2019,** *20* (8), 963-969.
12. Gold, M. R.; Reth, M. G., Antigen Receptor Function in the Context of the Nanoscale Organization of the B Cell Membrane. *Annu Rev Immunol* **2019,** *37*, 97-123.
13. Dintzis, H. M.; Dintzis, R. Z.; Vogelstein, B., Molecular Determinants of Immunogenicity: The Immunon Model of Immune Response. *Proc Natl Acad Sci U S A* **1976,** *73* (10), 3671-5.
14. Tittle, T. V.; Rittenberg, M. B., Igg B Memory Cell Subpopulations: Differences in Susceptibility to Stimulation by Ti-1 and Ti-2 Antigens. *J Immunol* **1980,** *124* (1), 202-6.
15. Obukhanych, T. V.; Nussenzweig, M. C., T-Independent Type Ii Immune Responses Generate Memory B Cells. *J Exp Med* **2006,** *203* (2), 305-10.
16. Vinuesa, C. G.; Chang, P. P., Innate B Cell Helpers Reveal Novel Types of Antibody Responses. *Nat Immunol* **2013,** *14* (2), 119-26.
17. Cerutti, A.; Cols, M.; Puga, I., Marginal Zone B Cells: Virtues of Innate-Like Antibody-Producing Lymphocytes. *Nat Rev Immunol* **2013,** *13* (2), 118-32.
18. Crotty, S., T Follicular Helper Cell Biology: A Decade of Discovery and Diseases. *Immunity* **2019,** *50* (5), 1132-1148.
19. Victora, G. D.; Nussenzweig, M. C., Germinal Centers. *Annu Rev Immunol* **2022,** *40*, 413-442.
20. Cyster, J. G.; Allen, C. D. C., B Cell Responses: Cell Interaction Dynamics and Decisions. *Cell* **2019,** *177* (3), 524-540.

21. Boyoglu-Barnum, S.; Ellis, D.; Gillespie, R. A.; Hutchinson, G. B.; Park, Y. J.; Moin, S. M.; Acton, O. J.; Ravichandran, R.; Murphy, M.; Pettie, D.; Matheson, N.; Carter, L.; Creanga, A.; Watson, M. J.; Kephart, S.; Ataca, S.; Vaile, J. R.; Ueda, G.; Crank, M. C.; Stewart, L.; Lee, K. K.; Guttman, M.; Baker, D.; Mascola, J. R.; Veesler, D.; Graham, B. S.; King, N. P.; Kanekiyo, M., Quadrivalent Influenza Nanoparticle Vaccines Induce Broad Protection. *Nature* **2021,** *592* (7855), 623-628.

22. Kanekiyo, M.; Wei, C. J.; Yassine, H. M.; McTamney, P. M.; Boyington, J. C.; Whittle, J. R.; Rao, S. S.; Kong, W. P.; Wang, L.; Nabel, G. J., Self-Assembling Influenza Nanoparticle Vaccines Elicit Broadly Neutralizing H1n1 Antibodies. *Nature* **2013,** *499* (7456), 102-6.

23. Kanekiyo, M.; Bu, W.; Joyce, M. G.; Meng, G.; Whittle, J. R.; Baxa, U.; Yamamoto, T.; Narpala, S.; Todd, J. P.; Rao, S. S.; McDermott, A. B.; Koup, R. A.; Rossmann, M. G.; Mascola, J. R.; Graham, B. S.; Cohen, J. I.; Nabel, G. J., Rational Design of an Epstein-Barr Virus Vaccine Targeting the Receptor-Binding Site. *Cell* **2015,** *162* (5), 1090-100.

24. Kanekiyo, M.; Joyce, M. G.; Gillespie, R. A.; Gallagher, J. R.; Andrews, S. F.; Yassine, H. M.; Wheatley, A. K.; Fisher, B. E.; Ambrozak, D. R.; Creanga, A.; Leung, K.; Yang, E. S.; Boyoglu-Barnum, S.; Georgiev, I. S.; Tsybovsky, Y.; Prabhakaran, M. S.; Andersen, H.; Kong, W. P.; Baxa, U.; Zephir, K. L.; Ledgerwood, J. E.; Koup, R. A.; Kwong, P. D.; Harris, A. K.; McDermott, A. B.; Mascola, J. R.; Graham, B. S., Mosaic Nanoparticle Display of Diverse Influenza Virus Hemagglutinins Elicits Broad B Cell Responses. *Nat Immunol* **2019,** *20* (3), 362-372.

25. Martinez-Murillo, P.; Tran, K.; Guenaga, J.; Lindgren, G.; Adori, M.; Feng, Y.; Phad, G. E.; Vazquez Bernat, N.; Bale, S.; Ingale, J.; Dubrovskaya, V.; O'Dell, S.; Pramanik, L.; Spangberg, M.; Corcoran, M.; Lore, K.; Mascola, J. R.; Wyatt, R. T.; Karlsson Hedestam, G. B., Particulate Array of Well-Ordered Hiv Clade C Env Trimers Elicits Neutralizing Antibodies That Display a Unique V2 Cap Approach. *Immunity* **2017,** *46* (5), 804-817 e7.

26. Akahata, W.; Yang, Z. Y.; Andersen, H.; Sun, S.; Holdaway, H. A.; Kong, W. P.; Lewis, M. G.; Higgs, S.; Rossmann, M. G.; Rao, S.; Nabel, G. J., A Virus-Like Particle Vaccine for Epidemic Chikungunya Virus Protects Nonhuman Primates against Infection. *Nat Med* **2010,** *16* (3), 334-8.

27. Arunachalam, P. S.; Walls, A. C.; Golden, N.; Atyeo, C.; Fischinger, S.; Li, C.; Aye, P.; Navarro, M. J.; Lai, L.; Edara, V. V.; Roltgen, K.; Rogers, K.; Shirreff, L.; Ferrell, D. E.; Wrenn, S.; Pettie, D.; Kraft, J. C.; Miranda, M. C.; Kepl, E.; Sydeman, C.; Brunette, N.; Murphy, M.; Fiala, B.; Carter, L.; White, A. G.; Trisal, M.; Hsieh, C. L.; Russell-Lodrigue, K.; Monjure, C.; Dufour, J.; Spencer, S.; Doyle-Meyers, L.; Bohm, R. P.; Maness, N. J.; Roy, C.; Plante, J. A.; Plante, K. S.; Zhu, A.; Gorman, M. J.; Shin, S.; Shen, X.; Fontenot, J.; Gupta, S.; O'Hagan, D. T.; Van Der Most, R.; Rappuoli, R.; Coffman, R. L.; Novack, D.; McLellan, J. S.; Subramaniam, S.; Montefiori, D.; Boyd, S. D.; Flynn, J. L.; Alter, G.; Villinger, F.; Kleanthous, H.; Rappaport, J.; Suthar, M. S.; King, N. P.; Veesler, D.; Pulendran, B., Adjuvanting a Subunit Covid-19 Vaccine to Induce Protective Immunity. *Nature* **2021,** *594* (7862), 253-258.

28. Cohen, A. A.; van Doremalen, N.; Greaney, A. J.; Andersen, H.; Sharma, A.; Starr, T. N.; Keeffe, J. R.; Fan, C.; Schulz, J. E.; Gnanapragasam, P. N. P.; Kakutani, L. M.; West, A. P., Jr.; Saturday, G.; Lee, Y. E.; Gao, H.; Jette, C. A.; Lewis, M. G.; Tan, T. K.; Townsend, A. R.; Bloom, J. D.; Munster, V. J.; Bjorkman, P. J., Mosaic Rbd Nanoparticles Protect against Challenge by Diverse Sarbecoviruses in Animal Models. *Science* **2022**, eabq0839.

29. Dalvie, N. C.; Rodriguez-Aponte, S. A.; Hartwell, B. L.; Tostanoski, L. H.; Biedermann, A. M.; Crowell, L. E.; Kaur, K.; Kumru, O. S.; Carter, L.; Yu, J.; Chang, A.; McMahan, K.; Courant, T.; Lebas, C.; Lemnios, A. A.; Rodrigues, K. A.; Silva, M.; Johnston, R. S.; Naranjo, C. A.; Tracey, M. K.; Brady, J. R.; Whittaker, C. A.; Yun, D.; Brunette, N.; Wang, J. Y.; Walkey, C.; Fiala, B.; Kar, S.; Porto, M.; Lok, M.; Andersen, H.; Lewis, M. G.; Love, K. R.; Camp, D. L.; Silverman, J. M.; Kleanthous, H.; Joshi, S. B.; Volkin, D. B.; Dubois, P. M.; Collin, N.; King, N. P.; Barouch, D. H.; Irvine, D. J.; Love, J. C., Engineered Sars-Cov-2 Receptor Binding Domain Improves Manufacturability in Yeast and Immunogenicity in Mice. *Proc Natl Acad Sci U S A* **2021,** *118* (38).

30. King, H. A. D.; Joyce, M. G.; Lakhal-Naouar, I.; Ahmed, A.; Cincotta, C. M.; Subra, C.; Peachman, K. K.; Hack, H. R.; Chen, R. E.; Thomas, P. V.; Chen, W. H.; Sankhala, R. S.; Hajduczki, A.; Martinez, E. J.; Peterson, C. E.; Chang, W. C.; Choe, M.; Smith, C.; Headley, J. A.; Elyard, H. A.; Cook, A.; Anderson, A.; Wuertz, K. M.; Dong, M.; Swafford, I.; Case, J. B.; Currier, J. R.; Lal, K. G.; Amare, M. F.; Dussupt, V.; Molnar, S.; Daye, S. P.; Zeng, X.; Barkei, E. K.; Alfson, K.; Staples, H. M.; Carrion, R.; Krebs, S. J.; Paquin-Proulx, D.; Karasavvas, N.; Polonis, V. R.; Jagodzinski, L. L.; Vasan, S.; Scott, P. T.; Huang, Y.; Nair, M. S.; Ho, D. D.; de Val, N.; Diamond, M. S.; Lewis, M. G.; Rao, M.; Matyas, G. R.; Gromowski, G. D.; Peel, S. A.; Michael, N. L.; Modjarrad, K.; Bolton, D. L., Efficacy and Breadth of Adjuvanted Sars-Cov-2 Receptor-Binding Domain Nanoparticle Vaccine in Macaques. *Proc Natl Acad Sci U S A* **2021,** *118* (38).
31. Joyce, M. G.; Chen, W. H.; Sankhala, R. S.; Hajduczki, A.; Thomas, P. V.; Choe, M.; Martinez, E. J.; Chang, W. C.; Peterson, C. E.; Morrison, E. B.; Smith, C.; Chen, R. E.; Ahmed, A.; Wieczorek, L.; Anderson, A.; Case, J. B.; Li, Y.; Oertel, T.; Rosado, L.; Ganesh, A.; Whalen, C.; Carmen, J. M.; Mendez-Rivera, L.; Karch, C. P.; Gohain, N.; Villar, Z.; McCurdy, D.; Beck, Z.; Kim, J.; Shrivastava, S.; Jobe, O.; Dussupt, V.; Molnar, S.; Tran, U.; Kannadka, C. B.; Soman, S.; Kuklis, C.; Zemil, M.; Khanh, H.; Wu, W.; Cole, M. A.; Duso, D. K.; Kummer, L. W.; Lang, T. J.; Muncil, S. E.; Currier, J. R.; Krebs, S. J.; Polonis, V. R.; Rajan, S.; McTamney, P. M.; Esser, M. T.; Reiley, W. W.; Rolland, M.; de Val, N.; Diamond, M. S.; Gromowski, G. D.; Matyas, G. R.; Rao, M.; Michael, N. L.; Modjarrad, K., Sars-Cov-2 Ferritin Nanoparticle Vaccines Elicit Broad Sars Coronavirus Immunogenicity. *Cell Rep* **2021,** *37* (12), 110143.
32. Yassine, H. M.; Boyington, J. C.; McTamney, P. M.; Wei, C. J.; Kanekiyo, M.; Kong, W. P.; Gallagher, J. R.; Wang, L.; Zhang, Y.; Joyce, M. G.; Lingwood, D.; Moin, S. M.; Andersen, H.; Okuno, Y.; Rao, S. S.; Harris, A. K.; Kwong, P. D.; Mascola, J. R.; Nabel, G. J.; Graham, B. S., Hemagglutinin-Stem Nanoparticles Generate Heterosubtypic Influenza Protection. *Nat Med* **2015,** *21* (9), 1065-70.
33. Jardine, J. G.; Ota, T.; Sok, D.; Pauthner, M.; Kulp, D. W.; Kalyuzhniy, O.; Skog, P. D.; Thinnes, T. C.; Bhullar, D.; Briney, B.; Menis, S.; Jones, M.; Kubitz, M.; Spencer, S.; Adachi, Y.; Burton, D. R.; Schief, W. R.; Nemazee, D., Priming a Broadly Neutralizing Antibody Response to Hiv-1 Using a Germline-Targeting Immunogen. *Science* **2015,** *349* (6244), 156-61.
34. Peabody, D. S.; Manifold-Wheeler, B.; Medford, A.; Jordan, S. K.; do Carmo Caldeira, J.; Chackerian, B., Immunogenic Display of Diverse Peptides on Virus-Like Particles of Rna Phage Ms2. *J Mol Biol* **2008,** *380* (1), 252-63.
35. Moon, J. J.; Suh, H.; Li, A. V.; Ockenhouse, C. F.; Yadava, A.; Irvine, D. J., Enhancing Humoral Responses to a Malaria Antigen with Nanoparticle Vaccines That Expand Tfh Cells and Promote Germinal Center Induction. *Proc Natl Acad Sci U S A* **2012,** *109* (4), 1080-5.
36. Walls, A. C.; Fiala, B.; Schafer, A.; Wrenn, S.; Pham, M. N.; Murphy, M.; Tse, L. V.; Shehata, L.; O'Connor, M. A.; Chen, C.; Navarro, M. J.; Miranda, M. C.; Pettie, D.; Ravichandran, R.; Kraft, J. C.; Ogohara, C.; Palser, A.; Chalk, S.; Lee, E. C.; Guerriero, K.; Kepl, E.; Chow, C. M.; Sydeman, C.; Hodge, E. A.; Brown, B.; Fuller, J. T.; Dinnon, K. H., 3rd; Gralinski, L. E.; Leist, S. R.; Gully, K. L.; Lewis, T. B.; Guttman, M.; Chu, H. Y.; Lee, K. K.; Fuller, D. H.; Baric, R. S.; Kellam, P.; Carter, L.; Pepper, M.; Sheahan, T. P.; Veesler, D.; King, N. P., Elicitation of Potent Neutralizing Antibody Responses by Designed Protein Nanoparticle Vaccines for Sars-Cov-2. *Cell* **2020,** *183* (5), 1367-1382 e17.
37. Hauser, B. M.; Sangesland, M.; St Denis, K. J.; Lam, E. C.; Case, J. B.; Windsor, I. W.; Feldman, J.; Caradonna, T. M.; Kannegieter, T.; Diamond, M. S.; Balazs, A. B.; Lingwood, D.; Schmidt, A. G., Rationally Designed Immunogens Enable Immune Focusing Following Sars-Cov-2 Spike Imprinting. *Cell Rep* **2022,** *38* (12), 110561.
38. Herzenberg, L. A.; Tokuhisa, T.; Herzenberg, L. A., Carrier-Priming Leads to Hapten-Specific Suppression. *Nature* **1980,** *285* (5767), 664-7.

39. Chackerian, B.; Durfee, M. R.; Schiller, J. T., Virus-Like Display of a Neo-Self Antigen Reverses B Cell Anergy in a B Cell Receptor Transgenic Mouse Model. *J Immunol* **2008,** *180* (9), 5816-25.
40. Alonso-Padilla, J.; Papp, T.; Kajan, G. L.; Benko, M.; Havenga, M.; Lemckert, A.; Harrach, B.; Baker, A. H., Development of Novel Adenoviral Vectors to Overcome Challenges Observed with Hadv-5-Based Constructs. *Mol Ther* **2016,** *24* (1), 6-16.
41. Zak, D. E.; Andersen-Nissen, E.; Peterson, E. R.; Sato, A.; Hamilton, M. K.; Borgerding, J.; Krishnamurty, A. T.; Chang, J. T.; Adams, D. J.; Hensley, T. R.; Salter, A. I.; Morgan, C. A.; Duerr, A. C.; De Rosa, S. C.; Aderem, A.; McElrath, M. J., Merck Ad5/Hiv Induces Broad Innate Immune Activation That Predicts Cd8(+) T-Cell Responses but Is Attenuated by Preexisting Ad5 Immunity. *Proc Natl Acad Sci U S A* **2012,** *109* (50), E3503-12.
42. Rothemund, P. W., Folding DNA to Create Nanoscale Shapes and Patterns. *Nature* **2006,** *440* (7082), 297-302.
43. Veneziano, R.; Ratanalert, S.; Zhang, K.; Zhang, F.; Yan, H.; Chiu, W.; Bathe, M., Designer Nanoscale DNA Assemblies Programmed from the Top Down. *Science* **2016,** *352* (6293), 1534.
44. Knappe, G. A.; Wamhoff, E. C.; Read, B. J.; Irvine, D. J.; Bathe, M., In Situ Covalent Functionalization of DNA Origami Virus-Like Particles. *ACS Nano* **2021,** *15* (9), 14316-14322.
45. Jun, H.; Wang, X.; Parsons, M. F.; Bricker, W. P.; John, T.; Li, S.; Jackson, S.; Chiu, W.; Bathe, M., Rapid Prototyping of Arbitrary 2d and 3d Wireframe DNA Origami. *Nucleic Acids Res* **2021,** *49* (18), 10265-10274.
46. Wamhoff, E. C.; Banal, J. L.; Bricker, W. P.; Shepherd, T. R.; Parsons, M. F.; Veneziano, R.; Stone, M. B.; Jun, H.; Wang, X.; Bathe, M., Programming Structured DNA Assemblies to Probe Biophysical Processes. *Annu Rev Biophys* **2019,** *48*, 395-419.
47. Shaw, A.; Hoffecker, I. T.; Smyrlaki, I.; Rosa, J.; Grevys, A.; Bratlie, D.; Sandlie, I.; Michaelsen, T. E.; Andersen, J. T.; Hogberg, B., Binding to Nanopatterned Antigens Is Dominated by the Spatial Tolerance of Antibodies. *Nat Nanotechnol* **2019,** *14* (2), 184-190.
48. Veneziano, R.; Moyer, T. J.; Stone, M. B.; Wamhoff, E. C.; Read, B. J.; Mukherjee, S.; Shepherd, T. R.; Das, J.; Schief, W. R.; Irvine, D. J.; Bathe, M., Role of Nanoscale Antigen Organization on B-Cell Activation Probed Using DNA Origami. *Nat Nanotechnol* **2020,** *15* (8), 716-723.
49. Li, S.; Jiang, Q.; Liu, S.; Zhang, Y.; Tian, Y.; Song, C.; Wang, J.; Zou, Y.; Anderson, G. J.; Han, J. Y.; Chang, Y.; Liu, Y.; Zhang, C.; Chen, L.; Zhou, G.; Nie, G.; Yan, H.; Ding, B.; Zhao, Y., A DNA Nanorobot Functions as a Cancer Therapeutic in Response to a Molecular Trigger in Vivo. *Nat Biotechnol* **2018,** *36* (3), 258-264.
50. Wang, Z.; Song, L.; Liu, Q.; Tian, R.; Shang, Y.; Liu, F.; Liu, S.; Zhao, S.; Han, Z.; Sun, J.; Jiang, Q.; Ding, B., A Tubular DNA Nanodevice as a Sirna/Chemo-Drug Co-Delivery Vehicle for Combined Cancer Therapy. *Angew Chem Int Ed Engl* **2021,** *60* (5), 2594-2598.
51. Liu, X.; Xu, Y.; Yu, T.; Clifford, C.; Liu, Y.; Yan, H.; Chang, Y., A DNA Nanostructure Platform for Directed Assembly of Synthetic Vaccines. *Nano Lett* **2012,** *12* (8), 4254-9.
52. Lucas, C. R.; Halley, P. D.; Chowdury, A. A.; Harrington, B. K.; Beaver, L.; Lapalombella, R.; Johnson, A. J.; Hertlein, E. K.; Phelps, M. A.; Byrd, J. C.; Castro, C. E., DNA Origami Nanostructures Elicit Dose-Dependent Immunogenicity and Are Nontoxic up to High Doses in Vivo. *Small* **2022,** *18* (26), e2108063.
53. Dai, L.; Gao, G. F., Viral Targets for Vaccines against Covid-19. *Nat Rev Immunol* **2021,** *21* (2), 73-82.
54. Kleanthous, H.; Silverman, J. M.; Makar, K. W.; Yoon, I. K.; Jackson, N.; Vaughn, D. W., Scientific Rationale for Developing Potent Rbd-Based Vaccines Targeting Covid-19. *NPJ Vaccines* **2021,** *6* (1), 128.
55. Walls, A. C.; Park, Y. J.; Tortorici, M. A.; Wall, A.; McGuire, A. T.; Veesler, D., Structure, Function, and Antigenicity of the Sars-Cov-2 Spike Glycoprotein. *Cell* **2020**.

450 56. Yuan, M.; Wu, N. C.; Zhu, X.; Lee, C. D.; So, R. T. Y.; Lv, H.; Mok, C. K. P.; Wilson, I. A.,
451 A Highly Conserved Cryptic Epitope in the Receptor Binding Domains of Sars-Cov-2 and Sars-
452 Cov. *Science* **2020,** *368* (6491), 630-633.
453 57. Bar-On, Y. M.; Flamholz, A.; Phillips, R.; Milo, R., Sars-Cov-2 (Covid-19) by the Numbers.
454 *Elife* **2020,** *9*.
455 58. Weaver, G. C.; Villar, R. F.; Kanekiyo, M.; Nabel, G. J.; Mascola, J. R.; Lingwood, D., In
456 Vitro Reconstitution of B Cell Receptor-Antigen Interactions to Evaluate Potential Vaccine
457 Candidates. *Nat Protoc* **2016,** *11* (2), 193-213.
458 59. Wu, Y.; Wang, F.; Shen, C.; Peng, W.; Li, D.; Zhao, C.; Li, Z.; Li, S.; Bi, Y.; Yang, Y.; Gong,
459 Y.; Xiao, H.; Fan, Z.; Tan, S.; Wu, G.; Tan, W.; Lu, X.; Fan, C.; Wang, Q.; Liu, Y.; Zhang, C.; Qi,
460 J.; Gao, G. F.; Gao, F.; Liu, L., A Noncompeting Pair of Human Neutralizing Antibodies Block
461 Covid-19 Virus Binding to Its Receptor Ace2. *Science* **2020,** *368* (6496), 1274-1278.
462 60. Hauser, B. M.; Sangesland, M.; Lam, E. C.; Denis, K. J. S.; Feldman, J.; Yousif, A. S.;
463 Caradonna, T. M.; Kannegieter, T.; Balazs, A. B.; Lingwood, D.; Schmidt, A. G., Engineered
464 Receptor Binding Domain Immunogens Elicit Pan-Sarbecovirus Neutralizing Antibodies Outside
465 the Receptor Binding Motif. *bioRxiv* **2021**.
466 61. Lingwood, D.; McTamney, P. M.; Yassine, H. M.; Whittle, J. R.; Guo, X.; Boyington, J. C.;
467 Wei, C. J.; Nabel, G. J., Structural and Genetic Basis for Development of Broadly Neutralizing
468 Influenza Antibodies. *Nature* **2012,** *489* (7417), 566-70.
469 62. Sangesland, M.; Ronsard, L.; Kazer, S. W.; Bals, J.; Boyoglu-Barnum, S.; Yousif, A. S.;
470 Barnes, R.; Feldman, J.; Quirindongo-Crespo, M.; McTamney, P. M.; Rohrer, D.; Lonberg, N.;
471 Chackerian, B.; Graham, B. S.; Kanekiyo, M.; Shalek, A. K.; Lingwood, D., Germline-Encoded
472 Affinity for Cognate Antigen Enables Vaccine Amplification of a Human Broadly Neutralizing
473 Response against Influenza Virus. *Immunity* **2019,** *51* (4), 735-749 e8.
474 63. Saunders, K. O.; Wiehe, K.; Tian, M.; Acharya, P.; Bradley, T.; Alam, S. M.; Go, E. P.;
475 Scearce, R.; Sutherland, L.; Henderson, R.; Hsu, A. L.; Borgnia, M. J.; Chen, H.; Lu, X.; Wu, N.
476 R.; Watts, B.; Jiang, C.; Easterhoff, D.; Cheng, H. L.; McGovern, K.; Waddicor, P.; Chapdelaine-
477 Williams, A.; Eaton, A.; Zhang, J.; Rountree, W.; Verkoczy, L.; Tomai, M.; Lewis, M. G.; Desaire,
478 H. R.; Edwards, R. J.; Cain, D. W.; Bonsignori, M.; Montefiori, D.; Alt, F. W.; Haynes, B. F.,
479 Targeted Selection of Hiv-Specific Antibody Mutations by Engineering B Cell Maturation. *Science*
480 **2019,** *366* (6470).
481 64. Jardine, J.; Julien, J. P.; Menis, S.; Ota, T.; Kalyuzhniy, O.; McGuire, A.; Sok, D.; Huang,
482 P. S.; MacPherson, S.; Jones, M.; Nieusma, T.; Mathison, J.; Baker, D.; Ward, A. B.; Burton, D.
483 R.; Stamatatos, L.; Nemazee, D.; Wilson, I. A.; Schief, W. R., Rational Hiv Immunogen Design to
484 Target Specific Germline B Cell Receptors. *Science* **2013,** *340* (6133), 711-6.
485 65. McGuire, A. T.; Hoot, S.; Dreyer, A. M.; Lippy, A.; Stuart, A.; Cohen, K. W.; Jardine, J.;
486 Menis, S.; Scheid, J. F.; West, A. P.; Schief, W. R.; Stamatatos, L., Engineering Hiv Envelope
487 Protein to Activate Germline B Cell Receptors of Broadly Neutralizing Anti-Cd4 Binding Site
488 Antibodies. *J Exp Med* **2013,** *210* (4), 655-63.
489 66. Corbett, K. S.; Moin, S. M.; Yassine, H. M.; Cagigi, A.; Kanekiyo, M.; Boyoglu-Barnum, S.;
490 Myers, S. I.; Tsybovsky, Y.; Wheatley, A. K.; Schramm, C. A.; Gillespie, R. A.; Shi, W.; Wang, L.;
491 Zhang, Y.; Andrews, S. F.; Joyce, M. G.; Crank, M. C.; Douek, D. C.; McDermott, A. B.; Mascola,
492 J. R.; Graham, B. S.; Boyington, J. C., Design of Nanoparticulate Group 2 Influenza Virus
493 Hemagglutinin Stem Antigens That Activate Unmutated Ancestor B Cell Receptors of Broadly
494 Neutralizing Antibody Lineages. *mBio* **2019,** *10* (1).
495 67. Ronsard, L.; Yousif, A. S.; Peabody, J.; Okonkwo, V.; Devant, P.; Mogus, A. T.; Barnes,
496 R. M.; Rohrer, D.; Lonberg, N.; Peabody, D.; Chackerian, B.; Lingwood, D., Engineering an
497 Antibody V Gene-Selective Vaccine. *Front Immunol* **2021,** *12*, 730471.
498 68. Voss, J. E.; Gonzalez-Martin, A.; Andrabi, R.; Fuller, R. P.; Murrell, B.; McCoy, L. E.;
499 Porter, K.; Huang, D.; Li, W.; Sok, D.; Le, K.; Briney, B.; Chateau, M.; Rogers, G.; Hangartner, L.;

Feeney, A. J.; Nemazee, D.; Cannon, P.; Burton, D. R., Reprogramming the Antigen Specificity of B Cells Using Genome-Editing Technologies. *Elife* **2019,** *8*.

69. Rappuoli, R., Glycoconjugate Vaccines: Principles and Mechanisms. *Sci Transl Med* **2018,** *10* (456).

70. Schumann, B.; Hahm, H. S.; Parameswarappa, S. G.; Reppe, K.; Wahlbrink, A.; Govindan, S.; Kaplonek, P.; Pirofski, L. A.; Witzenrath, M.; Anish, C.; Pereira, C. L.; Seeberger, P. H., A Semisynthetic Streptococcus Pneumoniae Serotype 8 Glycoconjugate Vaccine. *Sci Transl Med* **2017,** *9* (380).

71. Tian, J. H.; Patel, N.; Haupt, R.; Zhou, H.; Weston, S.; Hammond, H.; Logue, J.; Portnoff, A. D.; Norton, J.; Guebre-Xabier, M.; Zhou, B.; Jacobson, K.; Maciejewski, S.; Khatoon, R.; Wisniewska, M.; Moffitt, W.; Kluepfel-Stahl, S.; Ekechukwu, B.; Papin, J.; Boddapati, S.; Jason Wong, C.; Piedra, P. A.; Frieman, M. B.; Massare, M. J.; Fries, L.; Bengtsson, K. L.; Stertman, L.; Ellingsworth, L.; Glenn, G.; Smith, G., Sars-Cov-2 Spike Glycoprotein Vaccine Candidate Nvx-Cov2373 Immunogenicity in Baboons and Protection in Mice. *Nat Commun* **2021,** *12* (1), 372.

72. Heath, P. T.; Galiza, E. P.; Baxter, D. N.; Boffito, M.; Browne, D.; Burns, F.; Chadwick, D. R.; Clark, R.; Cosgrove, C.; Galloway, J.; Goodman, A. L.; Heer, A.; Higham, A.; Iyengar, S.; Jamal, A.; Jeanes, C.; Kalra, P. A.; Kyriakidou, C.; McAuley, D. F.; Meyrick, A.; Minassian, A. M.; Minton, J.; Moore, P.; Munsoor, I.; Nicholls, H.; Osanlou, O.; Packham, J.; Pretswell, C. H.; San Francisco Ramos, A.; Saralaya, D.; Sheridan, R. P.; Smith, R.; Soiza, R. L.; Swift, P. A.; Thomson, E. C.; Turner, J.; Viljoen, M. E.; Albert, G.; Cho, I.; Dubovsky, F.; Glenn, G.; Rivers, J.; Robertson, A.; Smith, K.; Toback, S.; nCo, V. S. G., Safety and Efficacy of Nvx-Cov2373 Covid-19 Vaccine. *N Engl J Med* **2021,** *385* (13), 1172-1183.

73. Huckriede, A.; Bungener, L.; Daemen, T.; Wilschut, J., Influenza Virosomes in Vaccine Development. *Methods Enzymol* **2003,** *373*, 74-91.

74. Morein, B.; Sundquist, B.; Hoglund, S.; Dalsgaard, K.; Osterhaus, A., Iscom, a Novel Structure for Antigenic Presentation of Membrane Proteins from Enveloped Viruses. *Nature* **1984,** *308* (5958), 457-60.

75. Garcia-Beltran, W. F.; Lam, E. C.; Astudillo, M. G.; Yang, D.; Miller, T. E.; Feldman, J.; Hauser, B. M.; Caradonna, T. M.; Clayton, K. L.; Nitido, A. D.; Murali, M. R.; Alter, G.; Charles, R. C.; Dighe, A.; Branda, J. A.; Lennerz, J. K.; Lingwood, D.; Schmidt, A. G.; Iafrate, A. J.; Balazs, A. B., Covid-19-Neutralizing Antibodies Predict Disease Severity and Survival. *Cell* **2021,** *184* (2), 476-488 e11.

76. Garcia-Beltran, W. F.; Lam, E. C.; St Denis, K.; Nitido, A. D.; Garcia, Z. H.; Hauser, B. M.; Feldman, J.; Pavlovic, M. N.; Gregory, D. J.; Poznansky, M. C.; Sigal, A.; Schmidt, A. G.; Iafrate, A. J.; Naranbhai, V.; Balazs, A. B., Multiple Sars-Cov-2 Variants Escape Neutralization by Vaccine-Induced Humoral Immunity. *Cell* **2021,** *184* (9), 2523.

77. Tokatlian, T.; Read, B. J.; Jones, C. A.; Kulp, D. W.; Menis, S.; Chang, J. Y. H.; Steichen, J. M.; Kumari, S.; Allen, J. D.; Dane, E. L.; Liguori, A.; Sangesland, M.; Lingwood, D.; Crispin, M.; Schief, W. R.; Irvine, D. J., Innate Immune Recognition of Glycans Targets Hiv Nanoparticle Immunogens to Germinal Centers. *Science* **2019,** *363* (6427), 649-654.

78. Tam, H. H.; Melo, M. B.; Kang, M.; Pelet, J. M.; Ruda, V. M.; Foley, M. H.; Hu, J. K.; Kumari, S.; Crampton, J.; Baldeon, A. D.; Sanders, R. W.; Moore, J. P.; Crotty, S.; Langer, R.; Anderson, D. G.; Chakraborty, A. K.; Irvine, D. J., Sustained Antigen Availability During Germinal Center Initiation Enhances Antibody Responses to Vaccination. *Proc Natl Acad Sci U S A* **2016,** *113* (43), E6639-E6648.

79. Wamhoff, E. C.; Romanov, A.; Huang, H.; Read, B. J.; Ginsburg, E.; Knappe, G. A.; Kim, H. M.; Farrell, N. P.; Irvine, D. J.; Bathe, M., Controlling Nuclease Degradation of Wireframe DNA Origami with Minor Groove Binders. *ACS Nano* **2022**.

80. Chandrasekaran, A. R., Nuclease Resistance of DNA Nanostructures. *Nat Rev Chem* **2021,** *5* (4), 225-239.

81. Lin-Shiao, E.; Pfeifer, W. G.; Shy, B. R.; Saffari Doost, M.; Chen, E.; Vykunta, V. S.; Hamilton, J. R.; Stahl, E. C.; Lopez, D. M.; Sandoval Espinoza, C. R.; Deyanov, A. E.; Lew, R. J.; Poirer, M. G.; Marson, A.; Castro, C. E.; Doudna, J. A., Crispr-Cas9-Mediated Nuclear Transport and Genomic Integration of Nanostructured Genes in Human Primary Cells. *Nucleic Acids Res* **2022,** *50* (3), 1256-1268.

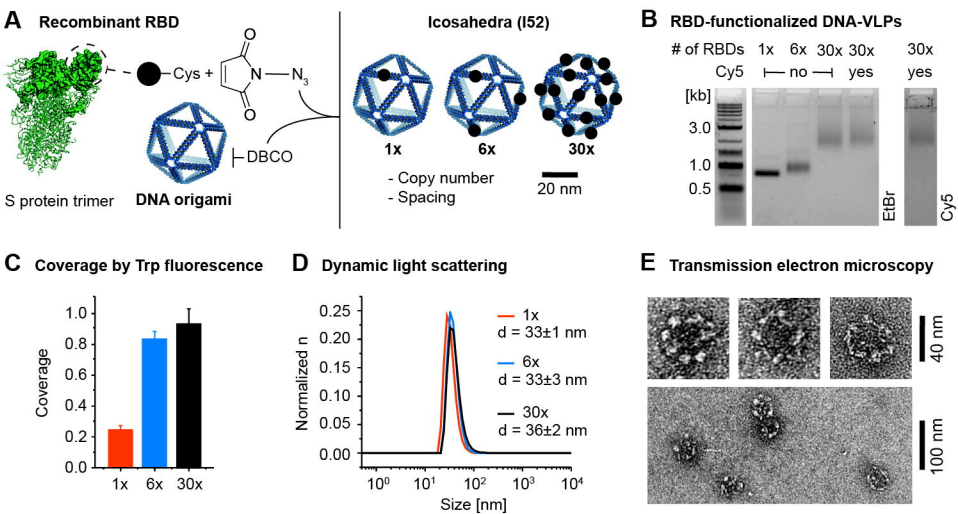
A
Recombinant RBD
Cys +
N
N3
O
O
DBCO
S protein trimer
DNA origami
Icosahedra (I52)
1x
6x
30x
- Copy number
- Spacing
20 nm
B
RBD-functionalized DNA-VLPs
# of RBDs 1x 6x 30x 30x
Cy5 no yes
30x
yes
[kb]
3.0
1.0
0.5
EtBr
Cy5
C
Coverage by Trp fluorescence
Coverage
1.0
0.8
0.6
0.4
0.2
0.0
1x 6x 30x
D
Dynamic light scattering
Normalized n
0.25
0.20
0.15
0.10
0.05
0.00
1x
d = 33±1 nm
6x
d = 33±3 nm
30x
d = 36±2 nm
Size [nm]
E
Transmission electron microscopy
40 nm
100 nm

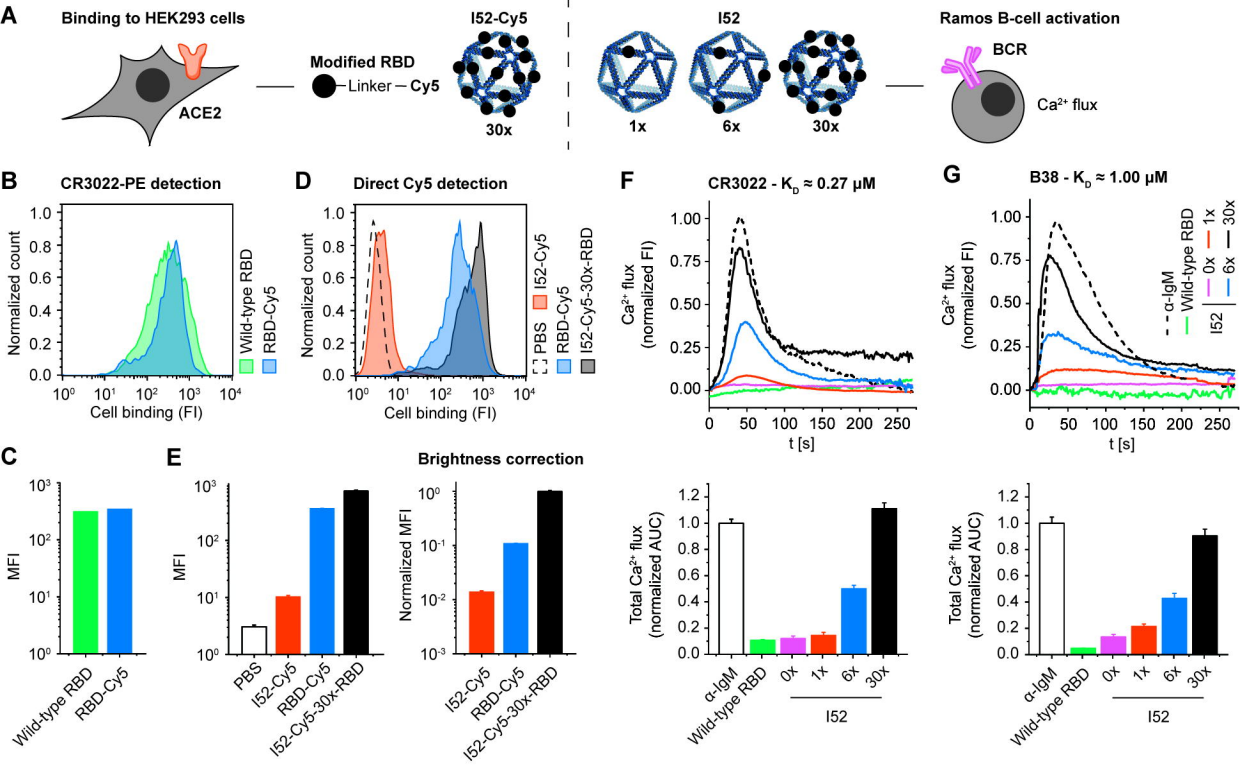
A
Binding to HEK293 cells
ACE2
Modified RBD
Linker – Cy5
I52-Cy5
30x
I52
1x
6x
30x
Ramos B-cell activation
BCR
Ca2+ flux
B
CR3022-PE detection
Normalized count
Cell binding (FI)
Wild-type RBD
RBD-Cy5
D
Direct Cy5 detection
PBS
I52-Cy5
RBD-Cy5
I52-Cy5-30x-RBD
F
CR3022 - KD ≈ 0.27 μM
Ca2+ flux (normalized FI)
t [s]
G
B38 - KD ≈ 1.00 μM
α-IgM
Wild-type RBD
I52
0x
1x
6x
30x
C
MFI
E
Brightness correction
Normalized MFI
Total Ca2+ flux (normalized AUC)

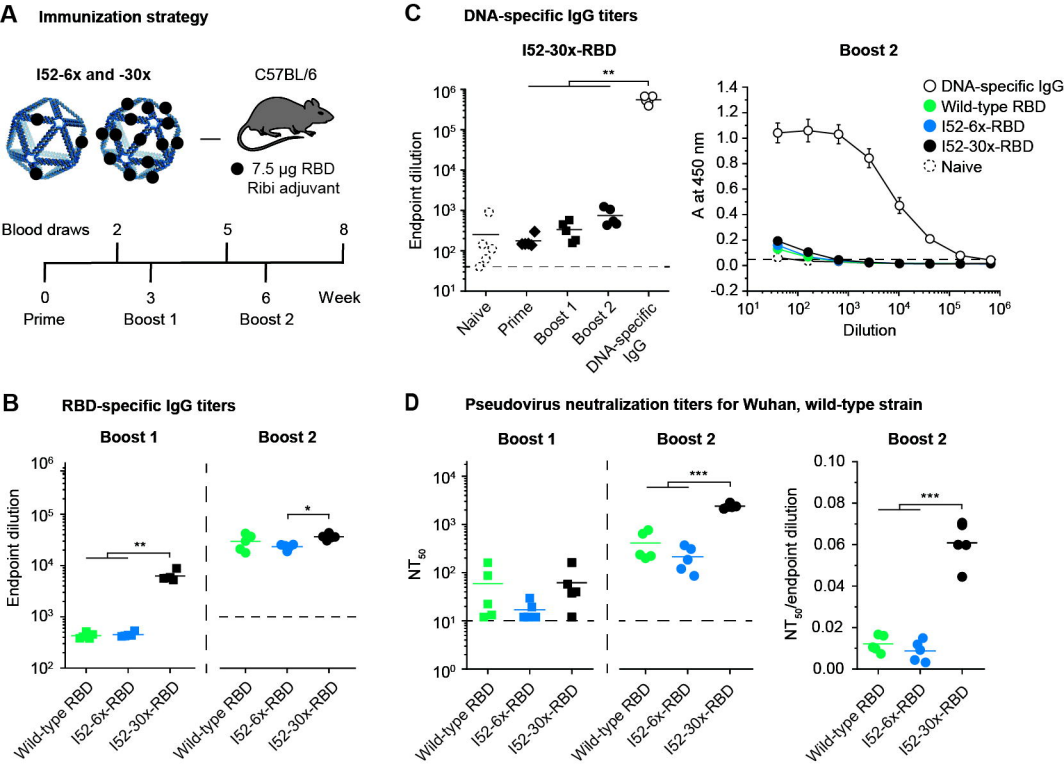
A
Immunization strategy
I52-6x and -30x
C57BL/6
7.5 µg RBD
Ribi adjuvant
Blood draws
2
5
8
0
3
6
Week
Prime
Boost 1
Boost 2
B
RBD-specific IgG titers
Boost 1
Boost 2
Endpoint dilution
Wild-type RBD
I52-6x-RBD
I52-30x-RBD
C
DNA-specific IgG titers
I52-30x-RBD
Boost 2
Endpoint dilution
Naive
Prime
Boost 1
Boost 2
DNA-specific IgG
A at 450 nm
Dilution
DNA-specific IgG
Wild-type RBD
I52-6x-RBD
I52-30x-RBD
Naive
D
Pseudovirus neutralization titers for Wuhan, wild-type strain
Boost 1
Boost 2
Boost 2
NT50
NT50/endpoint dilution
Wild-type RBD
I52-6x-RBD
I52-30x-RBD